Available online at www.sciencedirect.com
ScienceDirect
Polymer 48 (2007) 704–711
polymer
www.elsevier.com/locate/polymer

Core–shell nanohydrogel structures as tunable delivery systems

Nurettin Sahiner [a,*], Alina M. Alb [b], Richard Graves [c], Tarun Mandal [c], Gary L. McPherson [d], Wayne F. Reed [b], Vijay T. John [a,**]

[a] Department of Chemical and Biomolecular Engineering, Tulane University, New Orleans, LA 70118, USA
[b] Department of Physics, Tulane University, New Orleans, LA 70118, USA
[c] Department of Pharmacy, Xavier University of Louisiana College of Pharmacy, New Orleans, LA 70125, USA
[d] Department of Chemistry, Tulane University, New Orleans, LA 70118, USA

Received 21 September 2006; received in revised form 9 December 2006; accepted 12 December 2006
Available online 8 January 2007

Abstract

Poly(acrylonitrile-*co*-*N*-isopropylacrylamide) (p(AN-*co*-NIPAM)) core–shell hydrogel nanoparticles were synthesized by microemulsion polymerization and their feasibility as a drug carrier was investigated. Highly monodispersed nanoparticles with desired size range – i.e., 50–150 nm – were prepared by adjusting the reaction conditions. The hydrophobic core of the composite which consists primarily of poly(acrylonitrile), can be easily made highly hydrophilic by converting the nitrile groups to the corresponding amidoxime groups. This provides a level of tunability in the hydrophobicity/hydrophilicity balance of the composite nanoparticle. The thermo-responsive feature of the shell was utilized for the release of a model drug, propranolol (PPL). It is shown that the loading/release capacity of nanoparticles was increased almost two-fold by the amidoximation of the core material.
Published by Elsevier Ltd.

Keywords: Nanogel; Core–shell hydrogel; Nanodrug delivery systems

1. Introduction

We report a one-pot route for the synthesis of composite core–shell hydrogels with nanoscale dimensions and with tunable hydophilicity/hydrophobicity characteristics. Hydrogels are extremely useful as biomaterials and can be synthesized to be responsive for external stimuli [1,2]. Thermally responsive hydrogels such as poly(*N*-isopropylacrylamide) (p(NIPAM)) are of particular interest as they undergo temperature induced reversible coil to globule phase transitions at near physiological temperatures that influence their solubility characteristics [3–5]. Hydrogels with functional variants have been studied extensively, with recent reports describing their synthesis as submicron particles with a variety of hydrophobic and hydrophilic copolymers [6–11]. Hydrogels of nanosize are unique materials and can have numerous applications ranging from controlled release of active agents to sensor applications and can be used in bionanotechnology for variety of functions.

In this paper, we describe the synthesis of a hydrophobic/hydrophilic core–shell nanohydrogel system in a micellar system, with poly(*N*-isopropylacrylamide) as the shell, and poly(acrylonitrile) (p(AN)) as the hydrophobic core. Fig. 1 illustrates the concept wherein the hydrophobic/hydrophilic balance of the comonomer (NIPAM) is exploited by inducing access to the micelle palisade layer at synthetic conditions, while the hydrophobic monomer AN is resident in the interior of the micelles. The hypothesis is that the partitioning of the comonomers within the micelle will lead to a nonuniform distribution of the copolymer, with p(AN) constituting a core and p(NIPAM), the shell. While there is evidence for core–shell structures in the literature and we cite the especially interesting work by Lyon and Debord, much of the earlier work is essentially based on sequential processes where a hydrophobic

* Corresponding author.
** Corresponding author. Present address: Canakkale Onsekiz Mart University, Department of Chemistry, Terzioglu Campus, Canakkale 17020, Turkey.
E-mail address: sahiner@udel.edu (N. Sahiner).

0032-3861/$ - see front matter Published by Elsevier Ltd.
doi:10.1016/j.polymer.2006.12.014

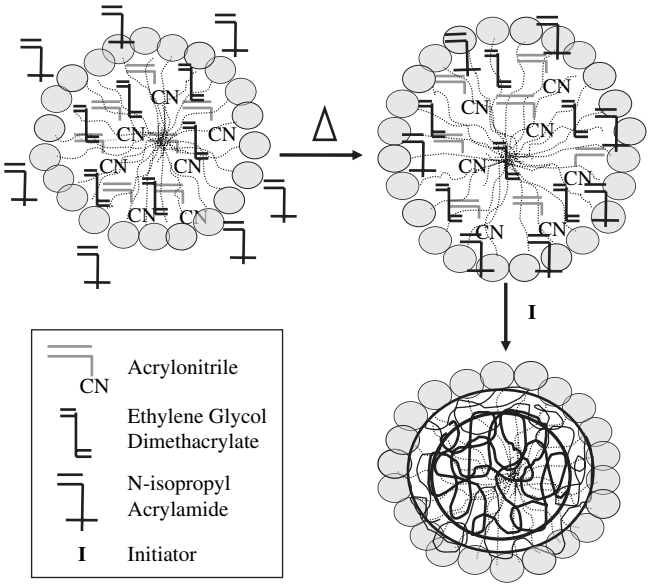

Fig. 1. A schematic of the copolymerization and simultaneous crosslinking reaction mechanism of acrylonitrile (AN) and *N*-isopropylacrylamide (NIPAM) in micelles.

core is subsequently covered by a hydrophilic shell [4]. There is an early and fascinating report by Pelton, on the one-pot synthesis of a p(NIPAM) shell–polystyrene core [6]. The work presented in this report extends the one-pot synthesis concept, and attempts to show an easy way in which the hydrophobic core material (p(AN)) can be selectively rendered hydrophilic by converting the nitrile groups to amidoxime groups at ambient temperature. Nanohydrogels prepared through this route are extremely monodispersed with a well-defined core–shell structure in the hydrophobic/hydrophilic composite of p(AN) and p(NIPAM) to a more diffused structure in the hydrophilic/hydrophilic composite of p(NIPAM) and amidoximated p(AN). We also report that independent nanoparticles of the hydrogels can be translated to interconnected beads of nanoparticles by adjusting the reaction conditions. The ability of these composite hydrogel systems to absorb and release a model drug species is described with the objective of demonstrating variable loading and release characteristics based on their tunable chemical functionalities.

2. Experimental section

2.1. Materials

The monomers used were *N*-isopropylacrylamide, (NIPAM), recrystallized from hexane, and acrylonitrile (AN). Ethylene glycol dimethacrylate, (EGDMA), was used as a crosslinker, and ammonium persulfate (APS) as the initiator. Sodium dodecyl sulfate (SDS) was the anionic surfactant used in micelle formulations and hydroxylamine hydrochloride for amidoximation reaction with propranolol (PPL) as the water-soluble drug used in model release studies. All chemicals were purchased from the Aldrich Chemical Company, Inc. (Milwaukee, Wisconsin).

2.2. Polymerization

Emulsion polymerization was used to prepare the composite polymer particles. In a typical one-pot one-to-one (1:1) mole ratio of AN to NIPAM core–shell nanohydrogel synthesis, 0.4 ml AN (6.076 mmol) was dissolved in 15 ml of 0.1 M SDS solution in water and 11.5 μl EGDMA was added (0.5 mol% with respect to total monomer amount). After vortex mixing, an equal amount of NIPAM (0.688 g) was added and the solution was mixed to obtain complete dissolution. The whole mixture was then placed in a temperature controlled water bath at 75 °C under constant stirring for 10 min and concurrent polymerization-crosslinking was initiated by the addition of 1 ml of 0.5 mol% (with respect to total monomer concentration) APS solution in water. The polymerization was carried out for at least 3.5 h. The monomer feed ratios were varied to obtain information on polymer particle size and morphology. All nanoparticles were purified by dialysis (Spectra/por 7 dialysis membrane, MWCO 10,000) by changing water daily for 14 days.

2.3. Nanostructure characterization

Transmission electron microscopy (TEM), scanning electron microscopy (SEM) and dynamic light scattering (DLS) techniques were used to get information about the morphology and the size of the nanoparticles. The purified nanoparticles were diluted in distilled water and a drop of suspension was placed on a formvar-coated copper TEM grid and dried overnight at ambient temperature. TEM micrographs were acquired using a JEOL JEM 2010 electron microscope operating at 200 kV. SEM images were obtained from a colloidal drop of suspension dried on aluminum stub at ambient temperature with 5 nm thickness gold sputtering and operating voltage of 10–15 kV.

The size, the deswelling behavior and the polydispersities of the hydrogel nanoparticles in distilled water were investigated via temperature controlled DLS. The measurements were performed with a detector angle of 90°, a Lexel 95 ion laser operating at a wavelength of 614 nm and a power of 100 mW was used as light source. The DLS technique allows the determination of the hydrodynamic diameter of a particle based on the relationship between the time dependent fluctuations in the intensity of the scattered light and the rate of diffusion of a particle in a solvent, via the usual Stokes–Einstein equation. The average hydrodynamic diameter of the particles at different temperatures was measured after equilibrating at each temperature for 15 min and followed by the measurements using 10–30 s integration times. At each temperature 5 consecutive runs were performed and the arithmetic average mean diameter was determined for each temperature.

The amidoximation reaction was verified via Fourier transform infrared radiation (FT-IR) spectroscopy with a Perkin–Elmer FT-IR System Spectrum GX. A drop of water with suspended particles was placed on a CaF_2 window. After evaporation of water in oven at 50 °C, the obtained thin film of particles on the FT-IR window placed in the sample holder

of the FT-IR instrument and the spectra were recorded against the background of CaF_2 window.

2.4. Amidoximation reaction and drug loading/release studies

In order to increase the hydrophilic character of the polymer particles, the nitrile groups of AN were converted to amidoxime groups [7]. In a typical amidoximation reaction, the nanogel solution was contacted with at least three-fold excess of NaOH neutralized hydroxylamine hydrochloride ($NH_2OH \cdot HCl$) followed by continuous stirring of the reaction mixture at ambient temperature for 2 days. After this time of the amidoximation reaction, the polymer particles were purified by exhaustive dialysis (MWCO 10,000, Spectra/Por membrane, Spectrum Laboratories, Rancho Dominguez, CA) against distilled water for 7 days by daily changing the extraction media. Drug loading was accomplished by placing the dialysis membrane containing polymer particles in 200 ml of a 0.2 mg/ml drug solution in water at 10 °C for 2 days, followed by the removal of the excess and unbound drug by a washing procedure. The dialysis membrane containing drug-loaded nanogel was soaked in chilled water (10 °C) for 2 days and the extraction medium was replaced every 6 h with pre-chilled fresh water. The release of the active agents was monitored continuously by UV detection at 290 and 305 nm which are the absorption maxima for PPL. A technique for continuous monitoring of drug release was used and included a pump circulating sample liquid through the detector train which comprised time dependent static light scattering (TDSLS), a home-built viscometer, refractive index (RI) and ultra-violet (UV) detectors [8,9].

3. Results and discussion

Fig. 1 is a schematic of the reaction scheme for the simultaneous polymerization and crosslinking of AN and NIPAM monomers in an oil-in-water microemulsion system. The amphiphilic structure of NIPAM provides its partitioning at the vicinity of the oil–water interface in SDS micelles. P(NIPAM) exhibits a well known thermo-responsive phase separation in aqueous solution with a lower critical solution temperature (LCST) of 32 °C [10]. Below this temperature, hydrogen bonding with water allows dissolution of polymer chains, while at temperatures above the LCST, the linear polymer adopts a globular conformation due to hydrophobic interactions [11]. The manifestation of the temperature induced volume phase transition of p(NIPAM) is the shrinkage of the crosslinked gels of the polymer when the temperature is raised above the cloud point [12].

Since the reactivity ratios for AN (1) and NIPAM (2) are relatively similar and both close to one ($r_1 = 0.863$ and $r_2 = 0.81$, respectively) [13], it was our hypothesis that the distribution of the polymeric components would be dependent on the partitioning of the monomers within the micelle. It was therefore anticipated that the hydrophobicity of AN and the amphiphilicity of NIPAM would lead to polymer particles with a greater concentration of AN moieties in the core, and an enhanced partitioning of NIPAM moieties to the particle exterior. Fig. 2 illustrates the morphologies of polymer particles obtained through the one-pot synthesis of p(AN-*co*-NIPAM) where the AN level is kept constant and the NIPAM level was systematically increased over an AN/NIPAM ratio 4:1 to 1:1. As the NIPAM level increases, the emergence of a shell is clearly observed. We attribute the shell to a region where it is almost exclusively occupied by p(NIPAM), due to the consequence of NIPAM polymerization towards the micelle surface, and almost solely AN polymerization in core. The particles are monodispersed with the size range in the order of 50–70 nm, and the shell width appears constant for particles of a given composition.

Fig. 3 illustrates the intriguing morphology of interconnected particles that are obtained by increasing the NIPAM level further (to a AN/NIPAM ratio 1:2). The particles are larger, in the order of 100–150 nm in diameter, and are polydispersed. While the interconnections between the particles

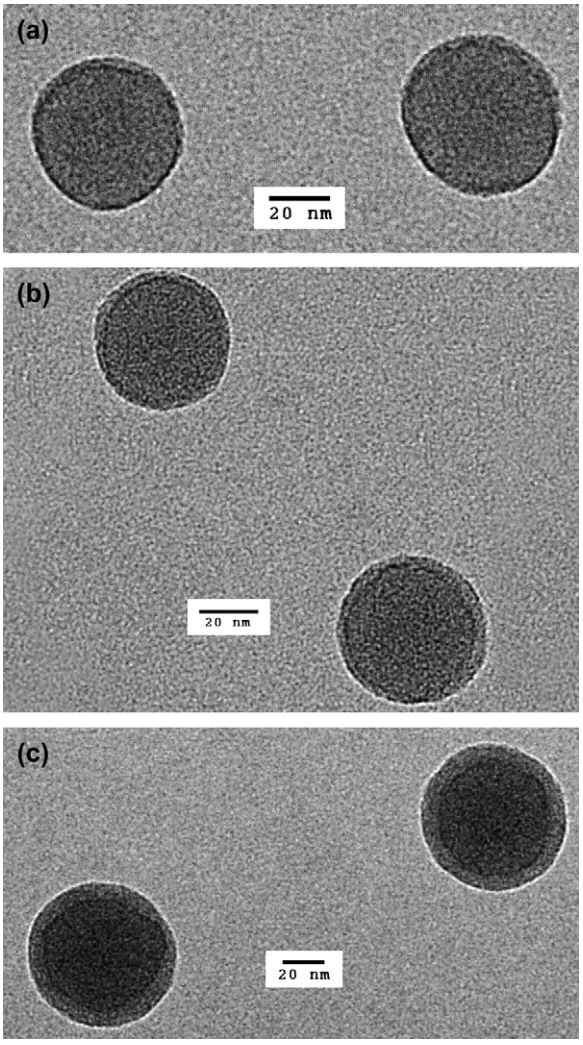

Fig. 2. TEM images of 0.5% ethylene glycol dimethacrylate (EGMA) crosslinked poly(AN-*co*-NIPAM) nanohydrogel at mole ratios of (a) 4:1, (b) 2:1, (c) 1:1. The scale bar is 20 nm.

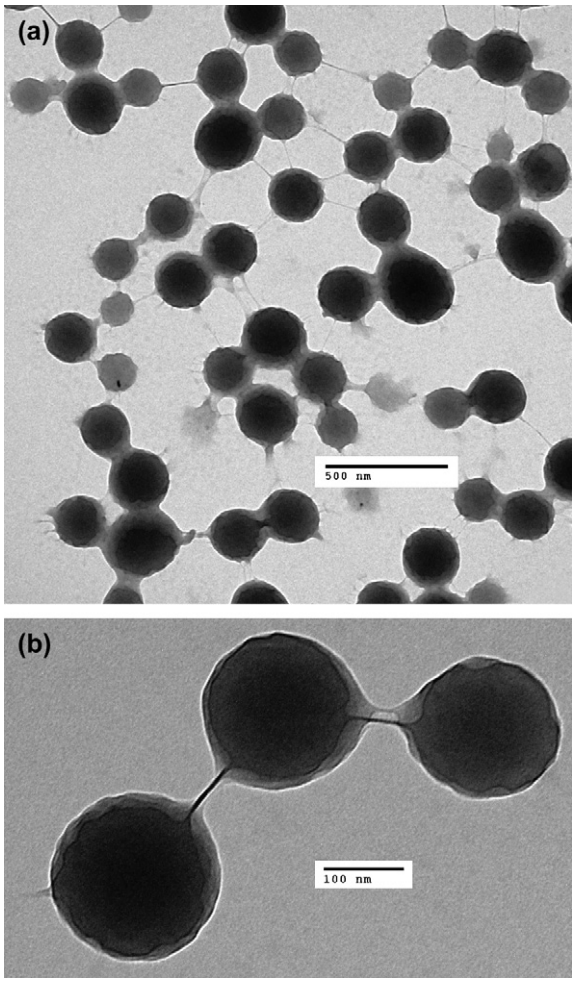

Fig. 3. TEM images of 0.5% crosslinked poly(AN-*co*-NIPAM) at a 1:2 mole ratio (a) and a higher resolution image of interconnected beads (b). The scale bar is 100 nm.

appear to be made up of the shell material p(NIPAM), the higher resolution images (Fig. 3(b)) show that there are several particles connected by core–shell type structures with a <10 nm diameter dense core, which is attributed to p(AN). Virtually all particles are interconnected, and there are a few particles that appear to be exclusively made up of the shell material (p(NIPAM)). The interconnection of particles may have useful applications in situations that require highly open and robust three-dimensional networks of hydrogel particles with high porosities allowing high throughput rates (e.g. chromatography, membranes). We explain the formation of these networks through the simple arguments of intradroplet polymerization kinetics competing against interdroplet polymerization kinetics, and the fact that the droplets are dynamic entities. Clearly, interdroplet polymerizations are more rapid, but during droplet collisions, interdroplet polymerization does occur to connect the particles. At the temperatures used in the synthesis (75 °C), the rapid motion of the droplets appears to minimize particle aggregation to clusters. Instead the interconnections between individual particles lead to an open long range network. Such interconnected networks, termed as microgels have been seen in a variety of other systems and have been reported extensively by Hoare and Pelton [14,5].

3.1. Amidoximated hydrogels

Modification of polymers with cyano groups is very attractive because the cyano groups can be readily converted to other useful derivatives such as amides, amines, amidoximes and carboxylic acids [15]. Amidoxime group containing polymers are very important in biological and environmental applications and can be obtained by conversion of the hydrophobic nitrile (cyano) groups to hydrophilic amidoxime groups [16,17]. To increase the hydrophilicity of the nanomaterial and impart additional functionality for bioconjugation, we have therefore converted the nitrile groups to the amidoxime groups through the simple procedure of adding NH_4OH at ambient conditions. The amidoximation reaction scheme is shown in Fig. 4.

Fig. 5 illustrates the FT-IR spectra of bare p(AN-*co*-NIPAM) and p(AN-*co*-NIPAM) subjected to 2 days amidoximation. The noteworthy feature is the band at about 2240 cm^{-1} which corresponds to nitrile groups on AN. With the amidoximation reaction the intensity of this band almost disappears whereas the intensity of amide I band at around 1650 cm^{-1} increases considerably. This increase is due to the newly formed –C=N in the amidoxime structure, which overlaps with the amide I and C=O band of secondary amide in p(NIPAM) structure. In addition, it is important to note that a newly formed broad N–O stretching vibration frequency at around 915 cm^{-1} can also be observed. Other peaks verified with library spectral information are consistent with the functional groups on both bare and amidoximated poly(AN-*co*-NIPAM) [16,18].

To visualize the progress of amidoximation reactions inside such core–shell particles, partially amidoximated p(AN-*co*-NIPAM) was removed during the amidoximation reaction and their TEM images were taken as depicted in Fig. 6(a). With the progress in the amidoximation reaction and increasing hydrophilicity of the core, the structure becomes more flexible and loose, additionally becoming more accessible to water molecules. Fig. 6(a) shows the TEM image of core–shell nanoparticles exposed to 25 min amidoximation reaction time. In comparison to the original structure of the nanoparticles (Fig. 2(c)), it is clear that the more diffused shell region

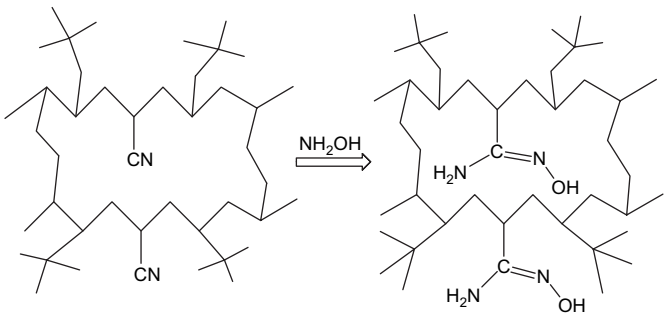

Fig. 4. Schematic of the amidoximation reaction mechanism of 0.5% crosslinked p(AN-*co*-NIPAM).

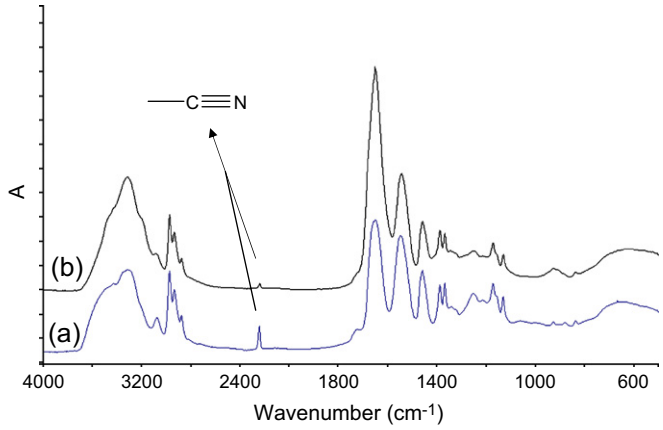

Fig. 5. FT-IR spectra of (a) bare and (b) amidoximated poly(AN-*co*-NIPAM).

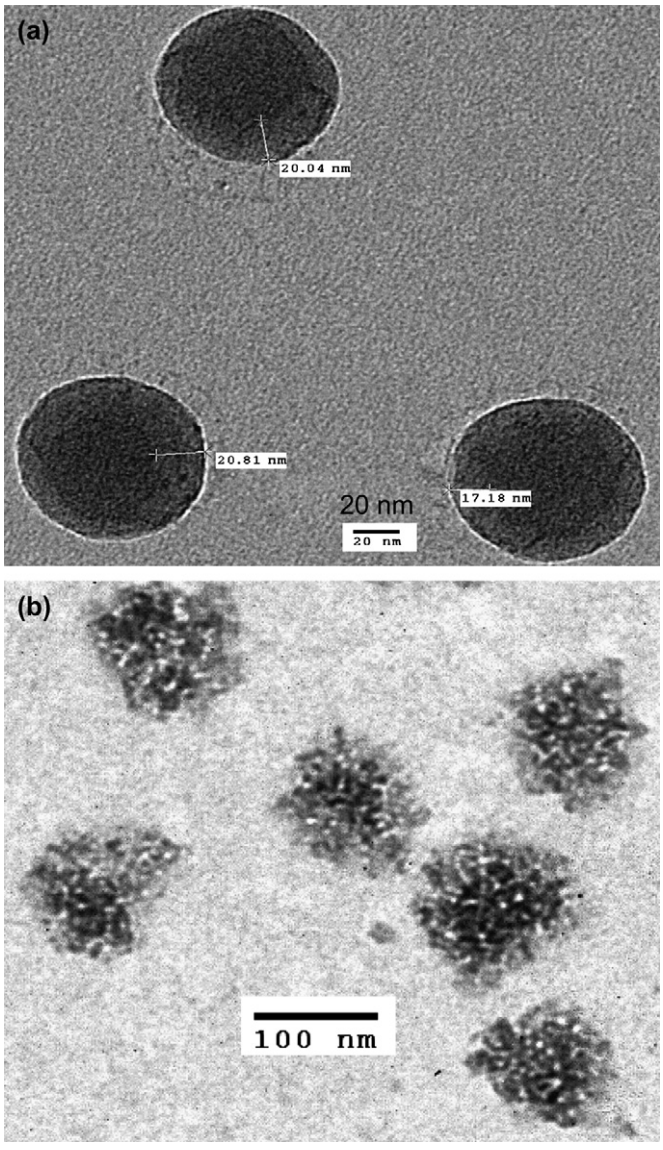

Fig. 6. Visualization of amidoximation reaction mechanism with TEM (a) after 25 min amidoximation reaction time. (b) Completely amidoximated p(AN-*co*-NIPAM) nanoparticles after 2 days amidoximation reaction at ambient temperature. The particles were stained with uranyl ions for enhanced contrast. Scale bars: (a) 20 nm, (b) 100 nm.

significantly increases to about 20 nm, although the center of the core continues to have a dense structure. The amidoximation reaction appears to proceed at a reaction front leading to a gradually shrinking core. Amidoximation for 2 days at ambient temperature appears to be sufficient for complete conversion of nitrile groups to amidoxime groups, as indicated by the disappearance of the nitrile peaks at 2240 cm^{-1}. The fully amidoximated structure is shown in Fig. 6(b), where we have stained the particles with uranyl ions to increase the contrast during imaging. A much more open and irregular particle structure is visualized. Amidoxime groups chelate strongly with uranyl ions, and the regions of enhancement in contrasting particularly in the particle interior in the TEM images (Fig. 6(b)), reflect regions of higher amidoxime group density. Fig. 7 depicts SEM images of connected p(AN-*co*-NIPAM) particles before (a) and after (b) amidoximation. The particles lose their spherical morphologies with amidoximation and are irregularly shaped.

Fig. 8(a) illustrates the dimensions of a single core–shell composite particle in the dry state, prepared at AN/NIPAM mole ratio of 1:1 whereas Fig. 8(b) illustrates the homopolymer of 0.5% crosslinked p(NIPAM) hydrogel particles obtained under the same reaction conditions. Fig. 8(c) is the graph of the swelling characteristics of these systems and

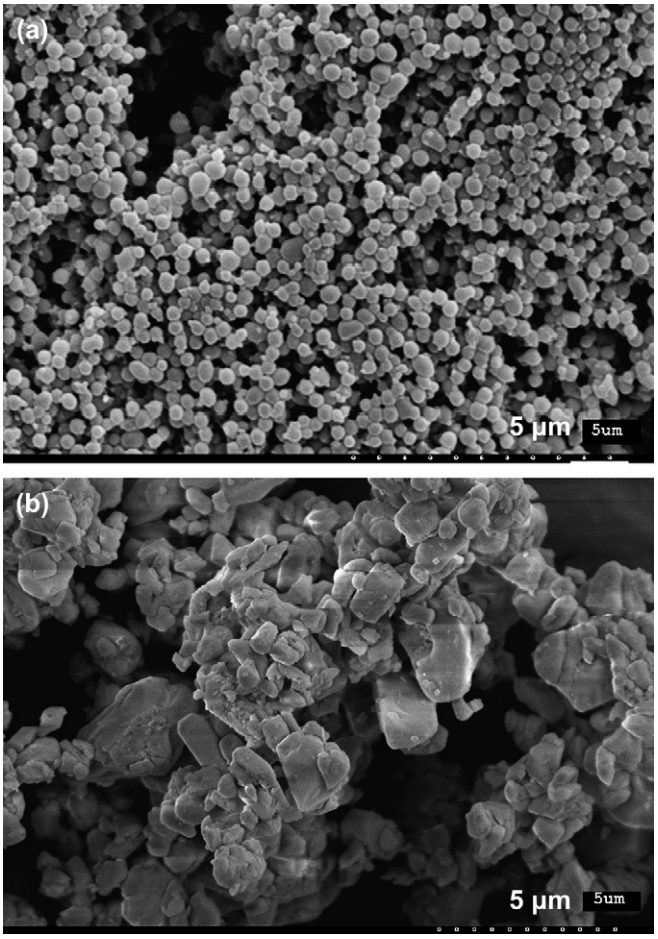

Fig. 7. SEM images of interconnected p(AN-*co*-NIPAM) with 1:2 mol ratio (a) before and (b) after the amidoximation reaction.

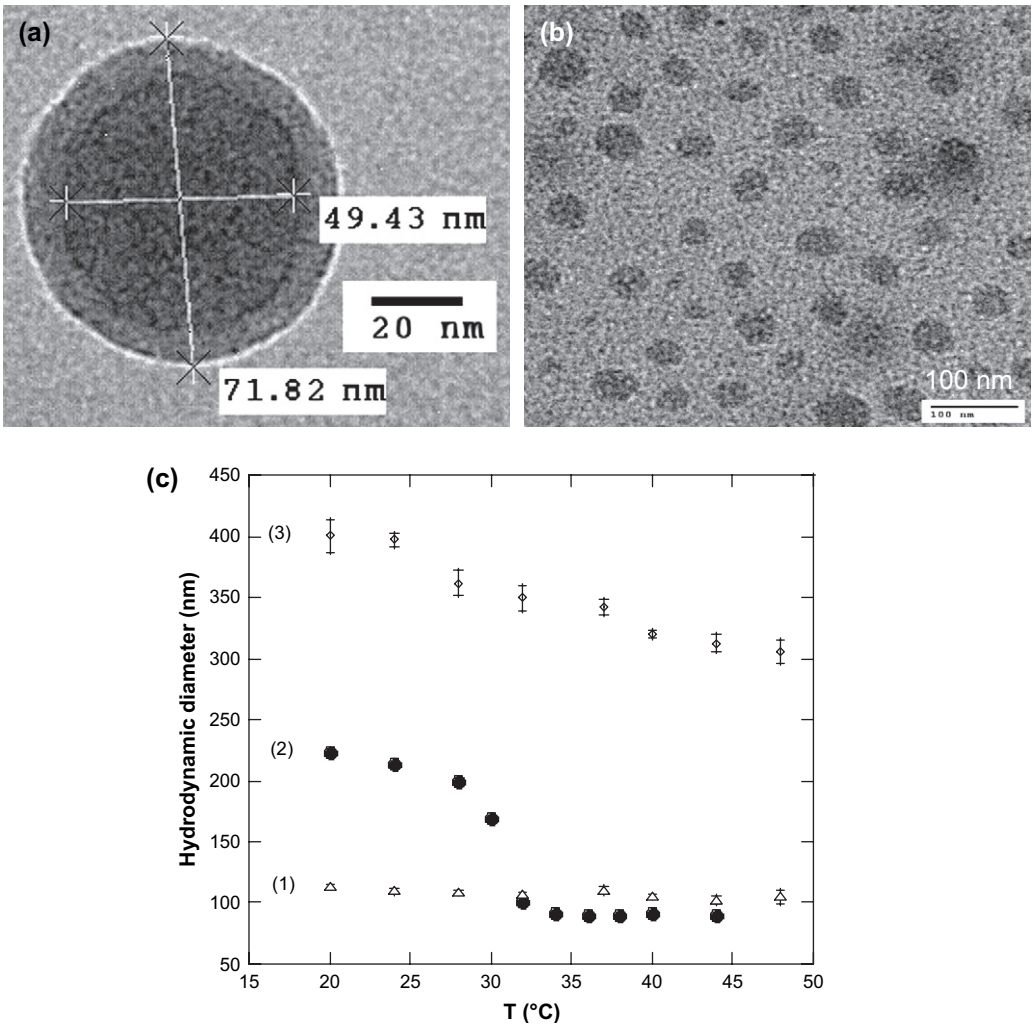

Fig. 8. TEM images of 0.5% crosslinked (a) p(AN-*co*-NIPAM) and (b) p(NIPAM). (c) Temperature dependence of hydrodynamic diameters of p(AN-*co*-NIPAM) (1), p(NIPAM) (2) and amidoximated p(AN-*co*-NIPAM) (3).

the amidoximated core–shell structure as a function of temperature as measured by DLS studies in water. The starting p(AN-*co*-NIPAM) particles are electrically neutral, except for the negligibly small amounts of residual persulfate initiator. The particles remain neutral upon amidoximation. The particles are denoted as (1), (2) and (3) for p(AN-*co*-NIPAM), p(NIPAM) and amidoximated p(AN-*co*-NIPAM), respectively. The TEM data for bare p(AN-*co*-NIPAM) can be compared to the DLS data. DLS indicates particles with hydrodynamic data of 110 nm, while the TEM data indicate a 71.8 nm particle with a hydrophobic core of 49.4 nm and a dry shell of 11.2 nm. If it is assumed that the swelling is entirely due to the p(NIPAM) in the shell, a rough calculation indicates that the shell increases to about 30 nm thickness upon hydration. The copolymer p(AN-*co*-NIPAM) ((1) in Fig. 8(c)) does not reveal any significant volume phase transition with temperature. A clear volume phase transition temperature for pure p(NIPAM) hydrogel (2) is 32 °C as observed, where it changes its dimensions from approximately 230 to 80 nm indicating a three-fold decrease in the diameter upon heating above LCST. Amidoximated p(AN-*co*-NIPAM) indicates a large swelling at around 400 nm, consistent with its hydrophilic structure. This swelling may be shell restricted as reported in studies of p(NIPAM-*co*-acrylic acid) copolymers [19]. The most important and useful feature of the amidoximated particles described here is the compression and broadening of the transition temperature upon heating above LCST of NIPAM. The amidoximated particles change their size almost 100 nm upon heating from 20 to 48 °C. This is a useful characteristic for specific applications, as demonstrated in the following drug release studies.

3.2. Drug release studies

To illustrate the applicability of this core–shell material as a controlled release vehicle, the absorption and release behaviors of the nanogel system were investigated using a water-soluble model drug, PPL (Fig. 9(a)), by means of the thermal responsive behavior of the nanogel. The loading of PPL was accomplished at 10 °C for 2 days and the *in situ* release was monitored at 37 °C via continuous UV monitoring. An UV (Shimadzu) detector was used to follow the PPL release via

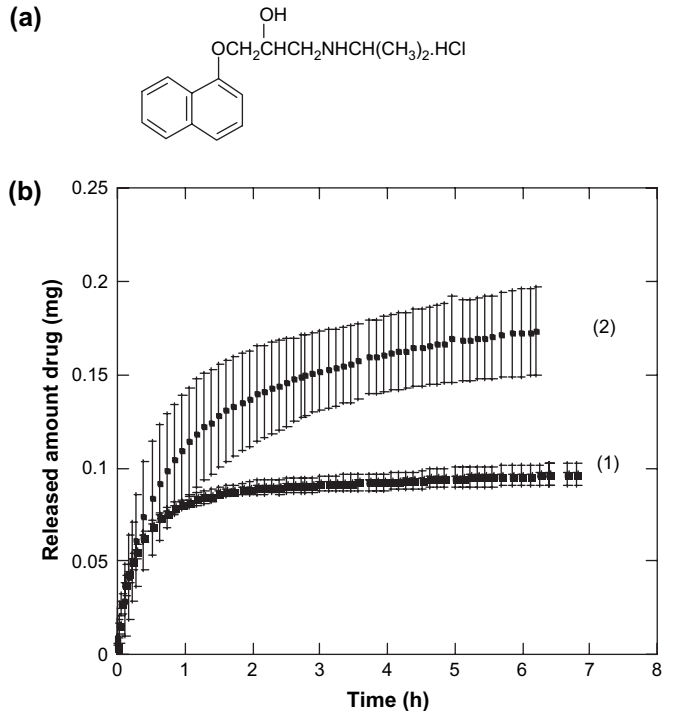

Fig. 9. (a) Chemical structure of a model drug propranolol (PPL) and (b) its release profile from p(AN-*co*-NIPAM) (1) and from amidoximated p(AN-*co*-NIPAM) (2) nanohydrogel systems at 37 °C.

its absorption at two different wavelengths, 290 and 305 nm, chosen based on the UV absorption spectrum of the drug. In each case, the p(AN-*co*-NIPAM) nanogel and its amidoximated version loaded with drug were introduced into a dialysis membrane (~10 ml) and immersed in a vessel with ~20 ml of water at 37 °C. An HPLC pump continuously recirculated the drug solution through the UV detector for several hours. The released amount of PPL in the p(AN-*co*-NIPAM) nanogel system as a function of time is shown in Fig. 9, and includes data from three separate measurements based on the UV absorbance at 290 nm. The 305 nm absorbance data yield identical results.

The release profile for both nanogels at 37 °C is shown in Fig. 9(b). Curve (1) illustrates the release characteristics of PPL from core–shell p(AN-*co*-NIPAM) and curve (2) the release characteristics from the amidoximated p(AN-*co*-NIPAM) nanogel system. Both release rate curves were fitted with first-order kinetics, yielding rate constants in the same range, $8.36 \times 10^{-5}\ s^{-1}$ for p(AN-*co*-NIPAM) and $9.78 \times 10^{-5}\ s^{-1}$ for the amidoximated p(AN-*co*-NIPAM). In order to verify that the kinetics correspond to the release from the nanogels, and not merely to the diffusion through the dialysis membrane, the control experiment was done where transport rates for pure PPL solution through the dialysis membrane were measured. The rate constant for the control experiment is $1.84 \times 10^{-4}\ s^{-1}$, twice higher than the rate constants for PPL release through the combined hydrogel + membrane system. We therefore assume that the slower and more prolonged release mechanism for both nanohydrogels is characteristic of the material and is due to PPL diffusion through the hydrogel. The data of Fig. 9 also illustrate the ability of the amidoximated structures to load and release a higher amount of drug. At 37 °C, both polymer components start to collapse (the temperature is above the LCST of p(NIPAM)) and initiate the release of PPL by discarding water. In the core–shell structure of p(AN-*co*-NIPAM) (1) only the shell (primarily NIPAM) contains PPL, whereas in the amidoximated nanoparticles, both core and shell materials are swollen and can encapsulate PPL leading to a significantly higher loading level. Although the release rate constants are similar, the amidoximated nanoparticles continue to release drug after the other system has reached its plateau.

4. Conclusions

The one-pot synthesis of p(AN-*co*-NIPAM) leads to a core–shell microgel structure with a well-defined shell that is primarily p(NIPAM). The interesting nature of the composite is the choice of the hydrophobic AN as the core material. Through simple amidoximation at ambient conditions, the AN functional groups can be converted to highly hydrophilic amidoxime groups. In principle therefore, the hydrophilicity/hydrophobicity of the composite material can be adjusted by the extent of amidoximation. Such features allow a degree of control over the loading levels of appropriate drug components. The broad range of temperature over which the volume changes can be further exploited to control burst release characteristics. There are interesting possibilities where the p(NIPAM) shell can be made to collapse at the p(NIPAM) LCST, providing a diffusional barrier to release from the hydrophilic core, and thus slowing down the release rates. The combination of adjusting the hydrophilicity/hydrophobicity balance to control the uptake capacity and the exploitation of the composite thermo-sensitivity has implications to the tenability of release. The facile nature of such synthesis is noteworthy.

Acknowledgements

Funding from National Science Foundation through grants 0438463 (VJ) and 0124006 (WR), and NASA NCC3-946, are gratefully acknowledged.

References

[1] Hoffman AS. Adv Drug Deliv Rev 2002;54:3–12.
[2] Miyata T, Uragami T, Nakamae K. Adv Drug Deliv Rev 2002;54:79–98.
[3] Pelton R. Macromol Symp 2004;207:57–65.
[4] Debord JD, Lyon LA. J Phys Chem B 2000;104:6327–31.
[5] Hoare T, Pelton R. Langmuir 2004;20:2123–33.
[6] Pelton RH. J Polym Sci Part A Polym Chem 1988;26:9–18.
[7] Sahiner N, Pekel N, Guven O. React Funct Polym 1999;39:139–46.
[8] Sorci GA, Reed WF. Langmuir 2002;18:353–64.
[9] Bayly EE, Brousseau J-L, Reed WF. Int J Polym Anal Charact 2002;7:1–18.
[10] Varghese S, Lele AK, Mashelkar RA. J Chem Phys 2000;112:3063–70.
[11] Principi T, Goh CCE, Liu RCW, Winnik FM. Macromolecules 2000;33:2958–66.
[12] Ma X, Huang X, Zhu L, Zhao X, Tang X. Polym Int 2005;54:83–9.

[13] Zhou G, Elaïssari A, Delair T, Pichot C. Colloid Polym Sci 1998;276: 1131–9.
[14] Hoare T, Pelton R. Macromolecules 2004;37:2544–50.
[15] Yu ZJ, Kang ET, Neoh KG. Langmuir 2002;18:10221–30.
[16] Sahiner N, Pekel N, Akkas P, Guven O. J Mater Sci Pure Appl Chem 2000;A37:1159–72.
[17] Lutfor MR, Silong S, Yunus WMZW, Rahman MZA, Ahmad MB, Haron MJ. J Chem Res Synop 2000;12:552–3.
[18] Silverstein MR, Webster XF. Spectrometric identification of organic compounds. 6th ed. New York: John Wiley & Sons Inc; 1998. p. 71–143 [chapter 3].
[19] Jones CD, Lyon LA. Langmuir 2003;19:4544–7.